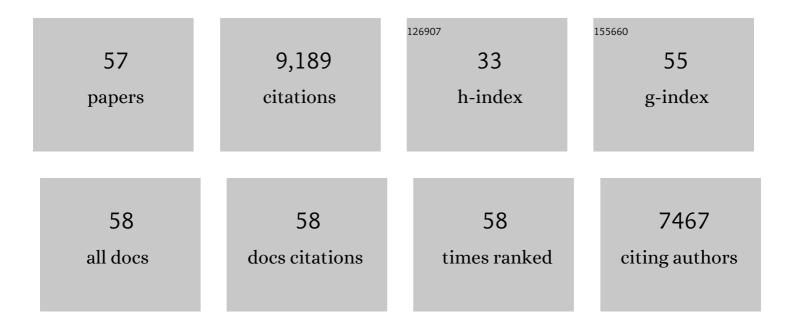
Yunhui Gong

List of Publications by Year in descending order

Source: https://exaly.com/author-pdf/12143197/publications.pdf Version: 2024-02-01



#	Article	IF	CITATIONS
1	Nonvolatile multilevel switching in artificial synaptic transistors based on epitaxial LiCoO2 thin films. Physical Review Materials, 2021, 5, .	2.4	2
2	Probing the Mechanical Properties of a Doped Li ₇ La ₃ Zr ₂ O ₁₂ Garnet Thin Electrolyte for Solid-State Batteries. ACS Applied Materials & Interfaces, 2020, 12, 24693-24700.	8.0	24
3	The Effects of Constriction Factor and Geometric Tortuosity on Liâ€lon Transport in Porous Solidâ€State Liâ€lon Electrolytes. Advanced Functional Materials, 2020, 30, 1910362.	14.9	22
4	Predicting the flexural strength of Liâ€ionâ€conducting garnet type oxide for solidâ€stateâ€batteries. Journal of the American Ceramic Society, 2020, 103, 5186-5195.	3.8	13
5	High-rate lithium cycling in a scalable trilayer Li-garnet-electrolyte architecture. Materials Today, 2019, 22, 50-57.	14.2	233
6	Flexible Solid-State Electrolyte with Aligned Nanostructures Derived from Wood. , 2019, 1, 354-361.		72
7	Evolution of Solid Oxide Fuel Cells via Fast Interfacial Oxygen Crossover. ACS Applied Energy Materials, 2019, 2, 4069-4074.	5.1	7
8	3D lithium metal anodes hosted in asymmetric garnet frameworks toward high energy density batteries. Energy Storage Materials, 2018, 14, 376-382.	18.0	114
9	Lithium-ion conductive ceramic textile: A new architecture for flexible solid-state lithium metal batteries. Materials Today, 2018, 21, 594-601.	14.2	134
10	Continuous plating/stripping behavior of solid-state lithium metal anode in a 3D ion-conductive framework. Proceedings of the National Academy of Sciences of the United States of America, 2018, 115, 3770-3775.	7.1	250
11	3Dâ€Printing Electrolytes for Solidâ€State Batteries. Advanced Materials, 2018, 30, e1707132.	21.0	236
12	Universal Soldering of Lithium and Sodium Alloys on Various Substrates for Batteries. Advanced Energy Materials, 2018, 8, 1701963.	19.5	186
13	Three-Dimensional, Solid-State Mixed Electron–Ion Conductive Framework for Lithium Metal Anode. Nano Letters, 2018, 18, 3926-3933.	9.1	175
14	Mixed ionic-electronic conductor enabled effective cathode-electrolyte interface in all solid state batteries. Nano Energy, 2018, 50, 393-400.	16.0	52
15	All-in-one lithium-sulfur battery enabled by a porous-dense-porous garnet architecture. Energy Storage Materials, 2018, 15, 458-464.	18.0	108
16	3D Microstructure Reconstruction and Characterization of Solid-State Electrolyte with Varying Porosity. Microscopy and Microanalysis, 2018, 24, 814-815.	0.4	0
17	All-wood, low tortuosity, aqueous, biodegradable supercapacitors with ultra-high capacitance. Energy and Environmental Science, 2017, 10, 538-545.	30.8	602
18	Reducing Interfacial Resistance between Garnetâ€Structured Solidâ€State Electrolyte and Liâ€Metal Anode by a Germanium Layer. Advanced Materials, 2017, 29, 1606042.	21.0	512

Yunhui Gong

#	Article	IF	CITATIONS
19	Garnet Solid Electrolyte Protected Li-Metal Batteries. ACS Applied Materials & Interfaces, 2017, 9, 18809-18815.	8.0	247
20	Three-dimensional bilayer garnet solid electrolyte based high energy density lithium metal–sulfur batteries. Energy and Environmental Science, 2017, 10, 1568-1575.	30.8	499
21	Toward garnet electrolyte–based Li metal batteries: An ultrathin, highly effective, artificial solid-state electrolyte/metallic Li interface. Science Advances, 2017, 3, e1601659.	10.3	647
22	Negating interfacial impedance in garnet-based solid-state Li metal batteries. Nature Materials, 2017, 16, 572-579.	27.5	1,583
23	Conformal, Nanoscale ZnO Surface Modification of Garnet-Based Solid-State Electrolyte for Lithium Metal Anodes. Nano Letters, 2017, 17, 565-571.	9.1	556
24	Transient Behavior of the Metal Interface in Lithium Metal–Garnet Batteries. Angewandte Chemie - International Edition, 2017, 56, 14942-14947.	13.8	227
25	Transient Behavior of the Metal Interface in Lithium Metal–Garnet Batteries. Angewandte Chemie, 2017, 129, 15138-15143.	2.0	12
26	<i>In Situ</i> Neutron Depth Profiling of Lithium Metal–Garnet Interfaces for Solid State Batteries. Journal of the American Chemical Society, 2017, 139, 14257-14264.	13.7	154
27	Stabilizing the Carnet Solid-Electrolyte/Polysulfide Interface in Li–S Batteries. Chemistry of Materials, 2017, 29, 8037-8041.	6.7	73
28	Rapid Thermal Annealing of Cathode-Garnet Interface toward High-Temperature Solid State Batteries. Nano Letters, 2017, 17, 4917-4923.	9.1	89
29	Transition from Superlithiophobicity to Superlithiophilicity of Garnet Solid-State Electrolyte. Journal of the American Chemical Society, 2016, 138, 12258-12262.	13.7	548
30	Flexible, solid-state, ion-conducting membrane with 3D garnet nanofiber networks for lithium batteries. Proceedings of the National Academy of Sciences of the United States of America, 2016, 113, 7094-7099.	7.1	769
31	Fabrication of organic-inorganic perovskite thin films for planar solar cells via pulsed laser deposition. AIP Advances, 2016, 6, 015001.	1.3	32
32	Promoting Electrocatalytic Activity of a Composite SOFC Cathode La _{0.8} Sr _{0.2} MnO _{3+δ} /Ce _{0.8} Gd _{0.2} O _{2-δMolten Carbonates. Journal of the Electrochemical Society, 2014, 161, F226-F232.}	ıb 2v9ith	13
33	Fast electrochemical CO2 transport through a dense metal-carbonate membrane: A new mechanistic insight. Journal of Membrane Science, 2014, 468, 373-379.	8.2	25
34	Surface modified silver-carbonate mixed conducting membranes for high flux CO2 separation with enhanced stability. Journal of Membrane Science, 2014, 453, 36-41.	8.2	32
35	Sr _{3â^'3x} Na _{3x} Si ₃ O _{9â^'1.5x} (x = 0.45) as a superior solid oxide-ion electrolyte for intermediate temperature-solid oxide fuel cells. Energy and Environmental Science, 2014, 7, 1680-1684.	30.8	75
36	Enhanced reversibility and durability of a solid oxide Fe–air redox battery by carbothermic reaction derived energy storage materials. Chemical Communications, 2014, 50, 623-625.	4.1	44

Yunhui Gong

37 38	A novel intermediate-temperature all ceramic iron–air redox battery: the effect of current density and cycle duration. RSC Advances, 2014, 4, 22621. An Allâ€Ceramic Solidâ€State Rechargeable Na ⁺ â€Battery Operated at Intermediate Temperatures. Advanced Functional Materials, 2014, 24, 5380-5384.	3.6	14
38	An Allâ€Ceramic Solidâ€State Rechargeable Na ⁺ â€Battery Operated at Intermediate Temperatures. Advanced Functional Materials, 2014, 24, 5380-5384.		
		14.9	52
39	Lattice-Boltzmann modeling of gas transport in Ni-Yttria-stabilized zirconia anodes during thermal cycling based on X-ray computed tomography. Electrochimica Acta, 2014, 121, 386-393.	5.2	5
40	Flux of silver-carbonate membranes for post-combustion CO2 capture: The effects of membrane thickness, gas concentration and time. Journal of Membrane Science, 2014, 455, 162-167.	8.2	25
41	Stabilizing Nanostructured Solid Oxide Fuel Cell Cathode with Atomic Layer Deposition. Nano Letters, 2013, 13, 4340-4345.	9.1	149
42	A new solid oxide molybdenum–air redox battery. Journal of Materials Chemistry A, 2013, 1, 14858.	10.3	32
43	Atomic Layer Deposition Functionalized Composite SOFC Cathode La _{0.6} Sr _{0.4} Fe _{0.8} Co _{0.2} O _{3-δ} -Gd _{0.2} Ce _{0.8} O _{1.9} : Enhanced Long-Term Stability. Chemistry of Materials. 2013. 25. 4224-4231.	6.7	73
44	Performance of Solid Oxide Iron-Air Battery Operated at 550°C. Journal of the Electrochemical Society, 2013, 160, A1241-A1247.	2.9	43
45	First spectroscopic identification of pyrocarbonate for high CO2 flux membranes containing highly interconnected three dimensional ionic channels. Physical Chemistry Chemical Physics, 2013, 15, 13147.	2.8	37
46	A high energy density all solid-state tungsten–air battery. Chemical Communications, 2013, 49, 5357.	4.1	43
47	Analysis of impact of sintering time on microstructure of LSM-YSZ composite cathodes by X-ray nanotomography. Materials Express, 2013, 3, 166-170.	0.5	6
48	Cyclic Durability of a Solid Oxide Fe-Air Redox Battery Operated at 650°C. Journal of the Electrochemical Society, 2013, 160, A1716-A1719.	2.9	32
49	Molten Carbonates as an Effective Oxygen Reduction Catalyst for 550–650°C Solid Oxide Fuel Cells. Journal of the Electrochemical Society, 2013, 160, F958-F964.	2.9	21
50	Energy storage characteristics of a new rechargeable solid oxide iron–air battery. RSC Advances, 2012, 2, 10163.	3.6	60
51	Quantitative analysis of micro structural and conductivity evolution of Ni-YSZ anodes during thermal cycling based on nano-computed tomography. Journal of Power Sources, 2011, 196, 10601-10605.	7.8	54
52	Performance of (La,Sr)MnO3 cathode based solid oxide fuel cells: Effect of bismuth oxide sintering aid in silver paste cathode current collector. Journal of Power Sources, 2011, 196, 928-934.	7.8	18
53	Analysis of the three-dimensional microstructure of a solid-oxide fuel cell anode using nano X-ray tomography. Journal of Power Sources, 2011, 196, 1915-1919.	7.8	72
54	Low temperature deposited (Ce,Gd)O2â^'x interlayer for La0.6Sr0.4Co0.2Fe0.8O3 cathode based solid oxide fuel cell. Journal of Power Sources, 2011, 196, 2768-2772.	7.8	24

#	Article	IF	CITATIONS
55	Preparation of YSZ films by magnetron sputtering for anode-supported SOFC. Solid State Ionics, 2011, 192, 413-418.	2.7	33
56	Effect of YSZ electrolyte surface modification on the performance of LSM/YSZ composite cathode. Solid State Ionics, 2011, 192, 505-509.	2.7	13
57	The study of the reconstructed three-dimensional structure of a solid-oxide fuel-cell cathode by X-ray nanotomography. Journal of Synchrotron Radiation, 2010, 17, 782-785.	2.4	16